Experimental investigation of taut leg moored FOWTs in damaged conditions

Experimental investigation of taut leg moored FOWTs in damaged conditions

F. Niosi, O. Dell'Edera, B. Paduano, G. Giorgi & G. Bracco
DIMEAS Dipartimento di Ingegneria Meccanica e Aerospaziale, Politecnico di Torino, Torino, Italy.

S. Schreier
Department of Maritime and Transport Technology, Delft University of Technology, Delft, Netherlands.

ABSTRACT: This study presents an experimental investigation focusing on the performance of a taut mooring systems for Floating Offshore Wind Turbines (FOWTs) under accidental limit state scenarios. These tests are part of the data obtained during the experimental campaign conducted at the Ship Hydromechanics Laboratory of Delft University of Technology, aimed to assess the behavior of FOWTs under various conditions, including operating, extreme, and failure scenarios. All the data related to the experiments are freely downloadable from this link. The experimental analysis conducted in this work focuses on simulating various failure scenarios, such as the rupture of mooring lines and turbine blade actuators considering two different mooring configurations. Results show that in such scenarios, taut mooring systems possess design characteristics that mitigate the risk of additional damage to the floating system and underscores the importance of understanding and mitigating risks associated with accidental limit states in offshore platforms, particularly by optimizing mooring configurations and materials to enhance overall safety and resilience.

1 INTRODUCTION

With the development of offshore wind technology, researchers are exploring various solutions for turbines, substructures, and mooring systems. Unlike turbines and substructures, which are not strongly dependent on the installation site, the mooring system needs to be customized based on seafloor type, bathymetry, and marine weather conditions. This study aims to experimentally test a non-conventional mooring solution of the taut type. The mooring is tested on the 5MW reference turbine defined by NREL in the report (Jonkman et al. 2009). The turbine is supported by the OC4 DeepCwind semi-submersible substructure, also developed by NREL laboratories and described in (Robertson et al. 2014). The design of the mooring system was carried out considering the installation of the turbine 3.45 nautical miles off the coast of Lampedusa, a small island located southwest of the coast of Sicily. Lampedusa was chosen because within the Green Deal agreement, Italy is actively participating in combating climate change and promoting the production of green energy including decarbonization efforts on minor islands like Lampedusa, which rely solely on locally produced electricity derived from fossil fuels. FOWTs, with their high energy density and consistent energy supply, stands as a promising solution for Lampedusa's energy transition. During the design of the mooring system and experimental tests, marine weather conditions were considered at the following coordinates: Latitude 35.570 deg N Longitude 12.498 deg E. Historical data for significant Wave Height (H_s), Peak Wave period (T_p), and Wind Speed (W_s) at 100m were downloaded for the last 50 years (tri-hourly sample) from ERA5 (ERA5) and post-processed to obtain an operational scatter and an Environmental Contour (EC). This allowed defining the test matrix for the experiments. In addition to environmental analysis events, tests were conducted to characterize the system dynamics, such as Free Decay Tests and multisine waves. This research seeks to examine the system behavior during an extreme event with a 100-year return period while the system has experienced a failure, designated as the Accidental Limit State (ALS). The study focuses on how the moored system responds under various damage scenarios, comparing cases with mooring lines made of constant stiffness springs and nylon with variable stiffness. The paper is organized as follows: first, a brief overview of the experimental setup is provided, including necessary details for replicating the experiment with a numerical model; then, the Ultimate Limit State (ULS) condition is defined through the EC

analysis; the experimental results are summarized in terms of frequency and time domain response; finally, conclusions are drawn, and possible improvements, limitations and future work are discussed.

2 EXPERIMENTAL SETUP

The experimental setup was designed to capture the motions of the structure, the tensions on the mooring lines, and the wave elevation at various points in space. A graphical representation of the setup is shown in Figure 1. All the tests were performed in head sea waves, recognizing that this can be assumed to be the critical condition for the mooring system (Paduano et al. 2024, Niosi et al. 2021). The mooring system analysed in this work is of taut type (Wang 2022) since it shows many advantages over conventional solutions (Bach-Gansmo et al. 2020). Given the scale of the experiment, 1:96, special attention is paid to identifying uncertainties by following the procedure recommended in (ITTC 2014). Despite the uncertainties being quantified and considered more than acceptable, it should be noted that to obtain results more representative of real conditions, future experimental campaigns will be conducted at a larger scale, in accordance with the dimensions of the facilities hosting the experiment.

2.1 *Substructure & Turbine*

The 1:96 scale model used in the experimental campaign was derived from the floating system composed of the 5MW turbine and the semisubmersible DeepCWind OC4 substructure (Robertson et al. 2014). The scaled model was constructed with careful consideration of the inertial and geometric properties of the full-scale system. The model is a single rigid body, depicted in Figure 2, representing the turbine and substructure assembly. Table 1 lists all the inertial characteristics of the model while in Figure 3 are reported all the geometric dimensions. The application of loads due to aerodynamic forces acting on the turbine is replicated using an actuator line connected to a fairlead placed at the same height as the nacelle (as shown in Figure 1). The actuator line replicates a constant thrust force whose magnitude is determined by scaling the nominal value of the turbine (Jonkman et al. 2009).

Table 1: Inertia Properties of the experimental model.

Parameter	Value	Unit of Measure
Mass	15.90	kg
I_{xx}	1.772	$kg \cdot m^2$
I_{yy}	1.788	$kg \cdot m^2$
I_{zz}	1.22	$kg \cdot m^2$
CoG from bottom	128	mm
Draft (Free-Floating)	208	mm

2.2 *Mooring System*

The mooring system consists of three lines offset by 120° from each other, and depending on the configuration, they are made of Nylon or Polyester with springs. In both cases, the load cells are positioned near the anchoring point on the seabed, as shown in Figures 4 and 6. Moreover, for both layouts, a turnbuckle is positioned along the line, allowing for the adjustment of the pretension value of the lines. The impact of the pre-tension value on the system's response depends on the axial stiffness characteristics of the lines under varying loading conditions, as stated in (Falkenberg et al. 2018). Since in this paper we focus on ALS condition, the mooring pretension varies among the tests when disconnecting a line. The line tensions are displayed in Section 5 so that it is possible to understand their impact on the structure dynamics. For both mooring configurations, the attachment and anchoring coordinates of each line are listed in Table 2 and referenced to the global reference system lying on the waterline and located at the center of the model.

Table 2: Fairleads and anchors position referred to the global reference system.

	$X(m)$	$Y(m)$	$Z(m)$
$Fairlead_1(F_1)$	0.213	0.369	-0.146
$Anchor_1(A_1)$	0.381	0.678	-1.042
$Fairlead_2(F_2)$	-0.426	0.000	-0.146
$Anchor_2(A_2)$	-0.781	0.000	-1.042
$Fairlead_3(F_3)$	0.213	-0.369	-0.146
$Anchor_3(A_3)$	0.381	0.678	-1.042

2.2.1 *Springs Mooring Layout*

In the mooring configuration where the lines are characterized by constant stiffness, springs are used connected in series to a polyester line. The polyester line, being much stiffer than the spring and connected in series with it, does not affect the stiffness of the line. The graphical representation of the mooring system with the Spring Layout Configuration (LCS) is shown in Figure 4 and the spring properties are reported in Table 3.

Table 3: Spring Characteristics.

Parameter	Value
Unstretched Length (mm)	52
Stiffness (N/m)	30.4
Max Load (N)	5.338
Wire Diameter (mm)	0.41
Supplier	Lee Spring (LeeSpring)
Part Number	LE 016B 11 M

2.2.2 *Nylon Mooring Layout*

On the other hand, in the Configuration Layout with Nylon lines (LCN), the system exhibits non-constant

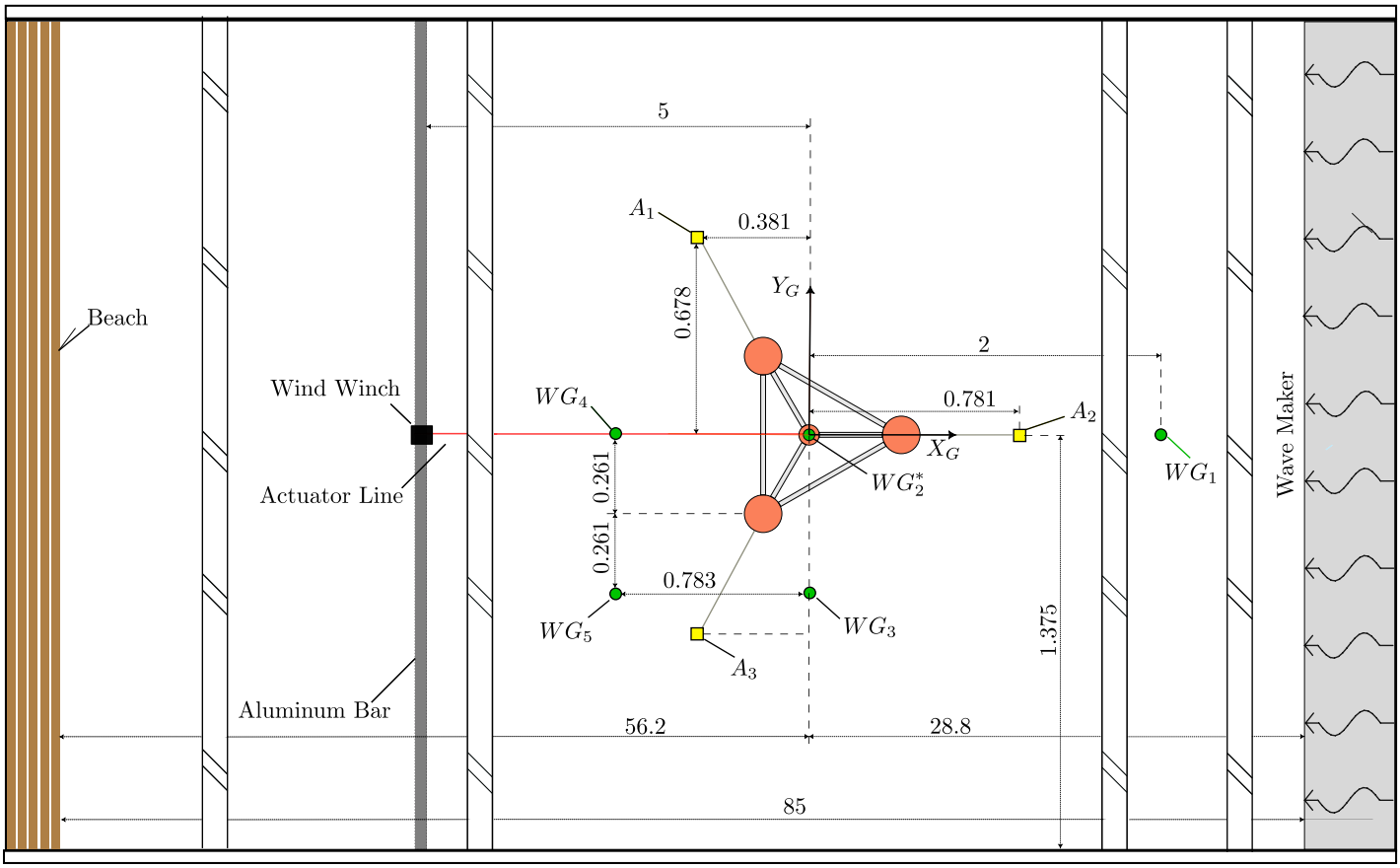

Figure 1: Graphical representation of experimental setup with Wave Gauges (WG_i), Anchor Points (A_i). The reported distances are expressed in mm.

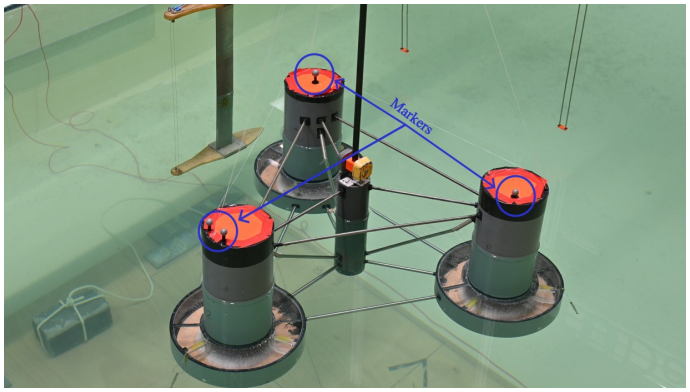

Figure 2: 1:96 small scale model of the DeepCWind 5MW Wind Turbine.

mooring stiffness. Indeed, nylon shows a variation in stiffness depending on the load it is subjected to. In this configuration, shown in Figure 6, the element that characterizes the stiffness of the line is precisely the nylon line. The mechanical characteristics of the line have been tested and examined in laboratory and reported in Figure 5. It is important to note that for the configuration with nylon mooring, the stiffness of the mooring lines does not precisely match the value obtained by scaling the full-scale model. This discrepancy arises from the difficulty in finding a nylon line that simultaneously matches both the stiffness and the maximum sustainable load. The results obtained with the nylon mooring system are intended solely to analyze the response of the mooring system with lines whose stiffness value is dependent on the ap-

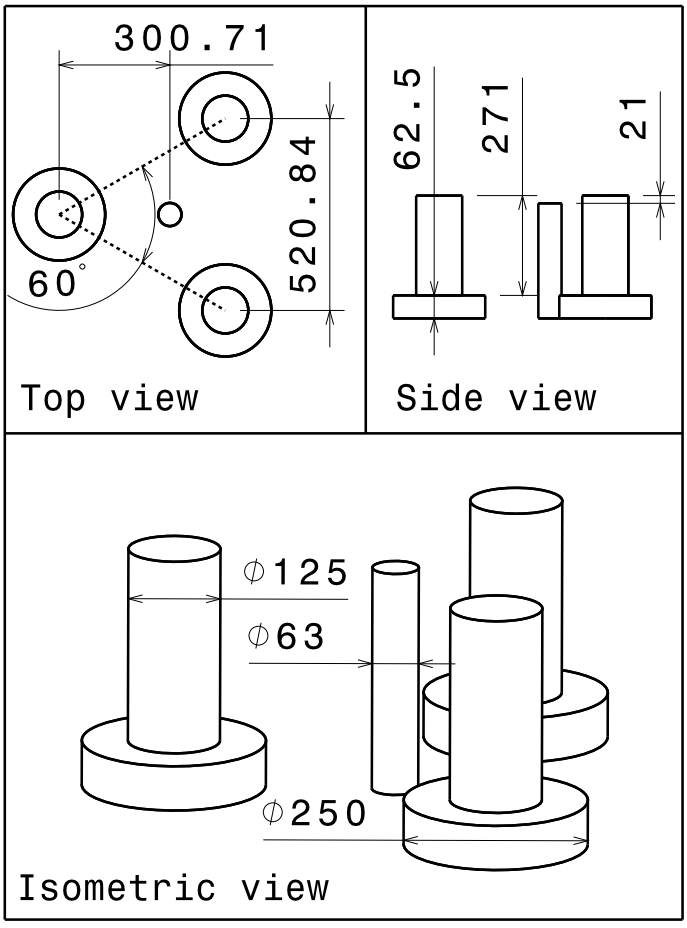

Figure 3: Dimensions of experimental model, Top view, Side view and Isometric view. All the quotes are in mm.

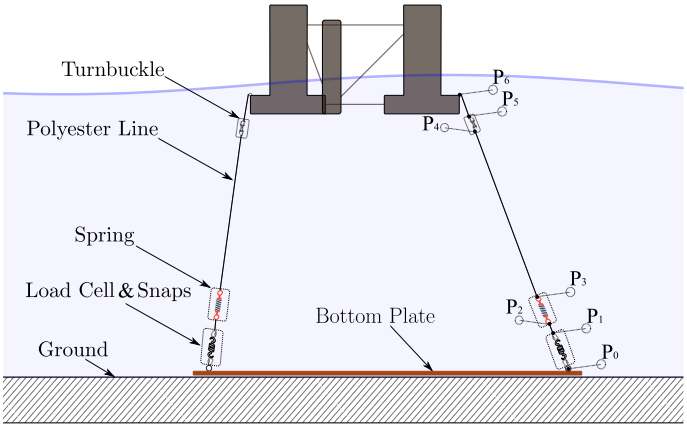

Figure 4: Mooring Layout Configuration using springs.

plied tension. Precisely scaling a mooring line with non-constant stiffness will be object of future works.

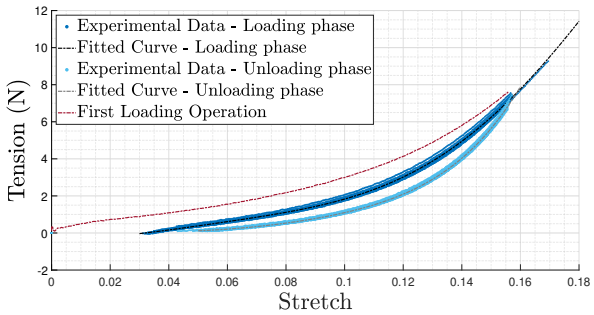

Figure 5: Traction test: tension vs stretch.

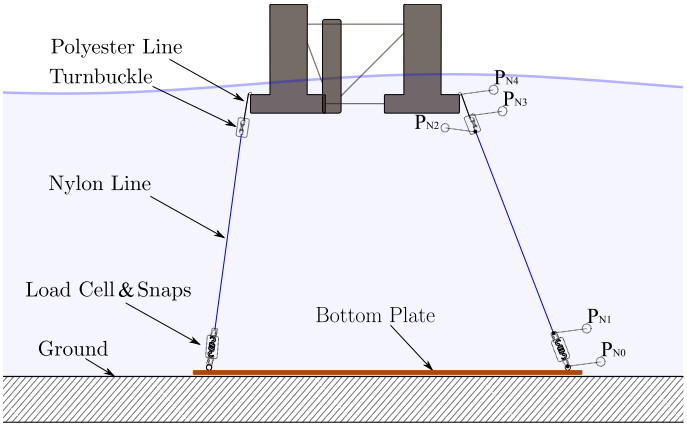

Figure 6: Mooring Layout Configuration using nylon lines.

3 SEA STATE DEFINITION

Knowing the site of installation, we gathered metocean data from the ERA5 database (Hersbach et al. 2020). With the three hours sampled data of H_s, T_p, W_s over a 50-year period, we were able to build the site-related EC according to the methodology suggested in (Veritas and Lloyd 2017). The resulting EC, depicted in Figure 7, allowed us to pinpoint the extreme event. To streamline testing and avoid excessive ULS-related tests, we conducted numerical simulations in Orcaflex ® environment (Orcina), revealing that the most severe system response occurs under conditions characterized by the maximum H_s since, in this EC, higher T_p values coincide with a sharp decrease in H_s, with the maximum period near the T_p associated with the maximum H_s. Following this procedure the utmost extreme event was selected to represent ULS and ALS conditions. The parameters of the selected sea state are reported in Table 4. The tests under damaged conditions simulated various failure scenarios, considering only one repetition of the wave.The ULS condition instead was tested considering 5 wave seeds. For sake of simplicity, in the next sections, only the same seed of the ALS conditions is reported.

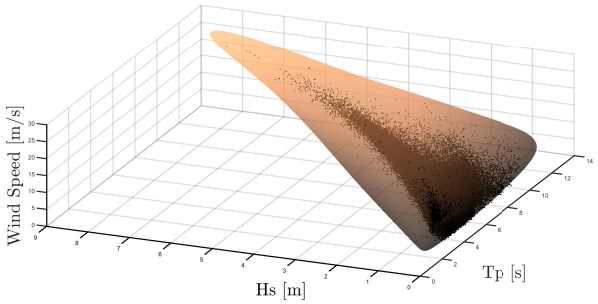

Figure 7: 3D Environmental Contour referred to the Lampedusa site.

Table 4: Definition of Extreme Sea State parameters. Full scale data and model scale data.

Parameter	Full Scale Data	Model Scale Data
H_s	8.27 m	86.2 mm
T_p	12.2 s	1.24 s
Spectrum	JONSWAP	JONSWAP
γ	3.3	3.3
W_s	28 m/s	/
Storm Duration (s)	3600	370

4 TEST MATRIX

The experimental tests analyzed in this article refer to a single extreme sea state. In the case of extreme events, the turbine is placed in safety conditions. In other words, the turbine blades are rotated 90 degrees to prevent lift, and the rotor is placed in parked conditions. In this case, the aerodynamic forces are solely related to the drag of the tower and the rotated blades and nacelle and can be neglected with respect the hydrodynamic loads.

The condition in which the turbine is in a safe state and everything functions according to design is defined as the Ultimate Limit State (ULS) condition, and the corresponding test is indicated by the acronym $117IWEXPRs04$. Here, the first number refers to the test number (defined in the citation), IW stands for Irregular Wave, EX stands for Extreme condition, PR for Parked Rotor, and $s04$ refers to the wave seed number.

When damage occurs to the substructure during the storm, this condition is defined as the ALS. Three types of damage were simulated:

- Damage Condition 1 (DC1): Simulates the breakage of the forward mooring line (i.e., mooring line 2).
- Damage Condition 2 (DC2): Simulates the breakage of one of the two stern lines (i.e., mooring line 3).
- Damage Condition 3 (DC3): Simulates the failure of the blade pitch actuation system, resulting in the blades remaining in the frontal position (0 degrees) and the rotor being locked.

The DC1 is simulated considering both configurations of mooring systems (LCS and LCN). All the others refer to the spring configuration. The test names definition is analogous to the ULS case, the only difference is that the ALS acronym defines the damaged condition and $N3$ stands to differentiate the nylon configuration. All the tests considered in this work are reported in Table 5 and their analyses discussed in the next section.

Table 5: ALS Test Matrix indicating Test ID, Test Name and Damage Conditions.

Test ID	Test Name	Damage Condition
117	$IW\ EX\ PR\ s04$	No Damage
154	$ALS\ EX\ PR\ s04$	DC 1
155	$ALS\ EX\ PR\ s04$	DC 2
156	$ALS\ EX\ s04$	DC 3
188	$ALS\ EX\ PR\ s04\ N3$	DC 1

5 PLATFORM RESPONSE IN EXTREME CONDITIONS

In this section, the results of the 5 extreme wave tests for the cases defined in Section 4 are compared and discussed. It is important to note that the system starts in a damaged condition before the start of the test. In future work, we want to analyze the phase of rupture during the test to provide insights into the transient phases of the system. In order to compare the results of the five tests effectively, it is imperative to ensure that the input wave in all cases is repeatable (ITTC 2014). For brevity and clarity, this paper presents the time history of the wave elevation measured by WG1 (position indicated in Figures 1) and reported in Figure 8. In the same figure, a zoom between 50 and 80s is reported. During this time interval, a wave peak occurs. The time histories of the five tests are synchronized in post-processing with respect to WG1, which serves as the undisturbed wave gauge unaffected by the presence of the floating structure. The motions and tensions are synchronized in the same manner and presented with the same visualization philosophy. Figure 9 depicts the time histories of the five tests for the three degrees of freedom of interest in head waves (surge, heave, and pitch). Figure 10 depicts the time histories of the tensions of the three mooring lines. Figure 12 depicts the dynamic frequency responses for the aforementioned tests obtained by considering the full-length time histories. The Single Side Spectrum Amplitude reported in the figure is computed as depicted in (Niosi et al. 2023). From this figure, it is possible to notice that the system exhibits a consistent response within the wave frequency range. However, notable alterations in system behavior are observed in the lower frequency range, particularly concerning surge and pitch motions. These changes manifest in different resonance periods and response amplitudes. In Tests 154 and 188, the absence of the bowline causes the pitch resonance to shift to lower frequencies. Conversely, the surge resonance period undergoes significant modification, resulting in the structure oscillating at frequencies lower than originally anticipated. Test 156, featuring a thrust force on the turbine, yields minimal differences except for a reduction in pitch oscillation around the resonance frequency. Figure 11 presents average values related to surge, pitch, and mooring line tensions. Test 117, serving as the reference, demonstrates nearly zero average values for surge and pitch due to intact lines with equal pre-tension values. Conversely, tests where the front mooring line is absent witness a reduction in pre-tension for the other two lines, inducing notable offsets in surge and pitch. This reduction in pre-tension, while preserving the frequency response, substantially mitigates the risk of further mooring failures. Test 155 exhibits a similar effect, albeit with the offset in the opposite direction and of smaller magnitude. Notably, Test 156 emerges as the most critical, with the average tension of the bowline increasing by over 40%, accompanied by substantial offset values. It is crucial to highlight that the thrust applied in Test 156 was computed using Orcaflex ® (Orcina), with the blades locked at 0° and the rotor brake engaged.

6 CONCLUSIONS & FUTURE WORKS

In this study, the dynamic response of a semi-submersible platform supporting a 5MW turbine under extreme conditions is experimentally analyzed. The behavior of the moored system is investigated under the assumption that it operates according to the project conditions, where all mooring lines are connected to the substructure, the turbine blades are rotated at 90 degrees, and the rotor is braked. Under these conditions, the motions of the structure are limited, and the mooring tensions remain within design limits. Subsequently, the scenario of a broken mooring line at the bow is simulated. It is observed that the turbine motions substantially increase, while the tensions on the mooring lines decrease. This ef-

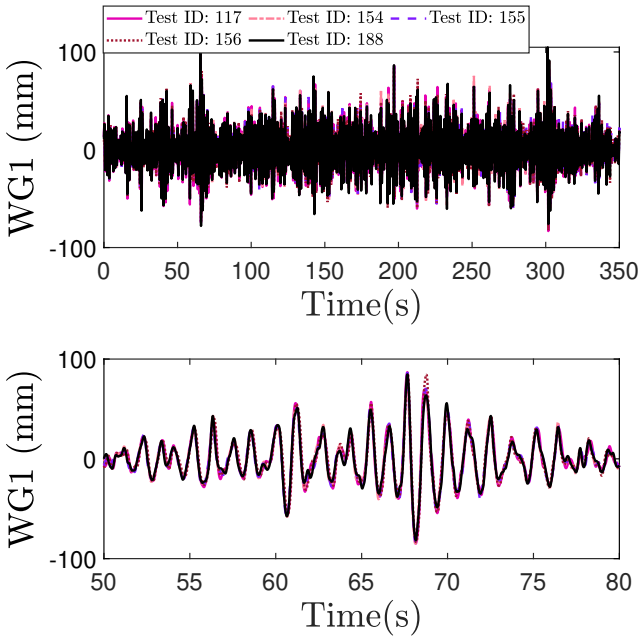

Figure 8: Wave Elevation at Wave Gauge 1. At the top of the figure, the full time histories of each test are reported, while in the bottom is a zoom of 30s.

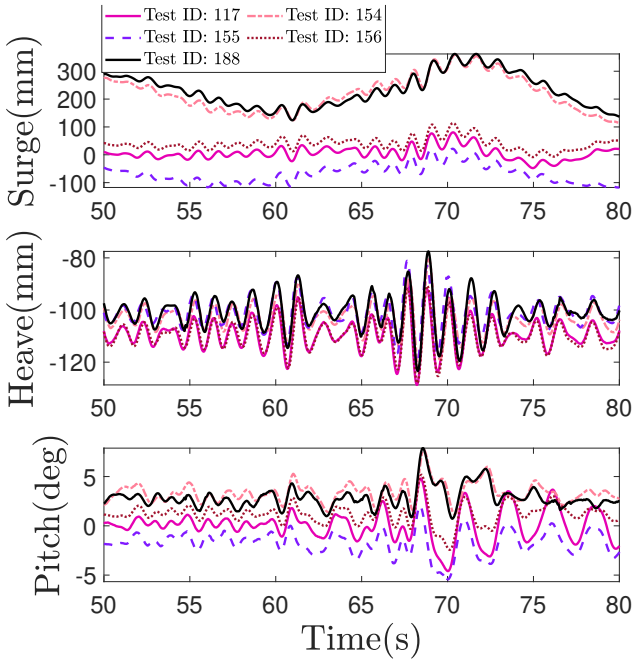

Figure 9: Time histories of Surge, Heave and Pitch motions for the five tested condition.

fect occurs because a taut mooring system is being used. When one mooring line is disconnected, the pre-tension value decreases, preventing the system from encountering another potential failure. Therefore, as long as the total motions of the structure remain within the maximum limits, this type of mooring system provides the opportunity to avoid redundant lines since the system automatically enters a "safety" condition. Similar conclusions can be drawn in the event of a rupture of one of the two stern lines except that the motions of the structure do not increase significantly in this case. Several considerations arise when simulating the rupture of the turbine blade actuators. In this case, a significant increase in tension on the bow line is observed, posing the risk of poten-

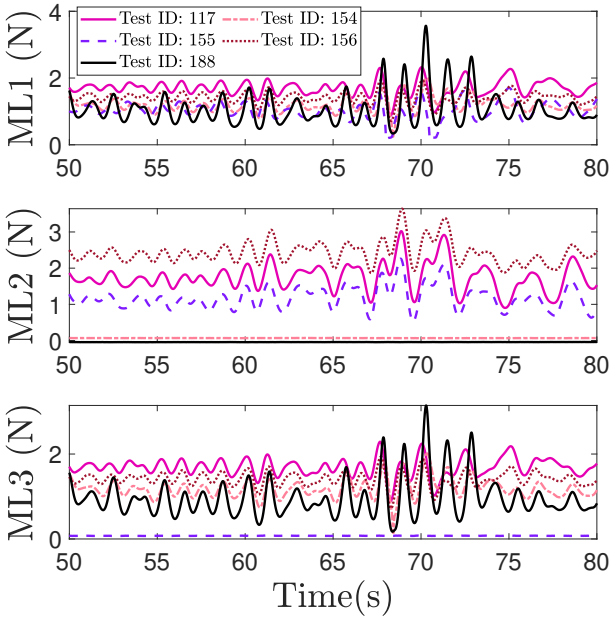

Figure 10: Time histories of mooring lines tensions for the five tested condition.

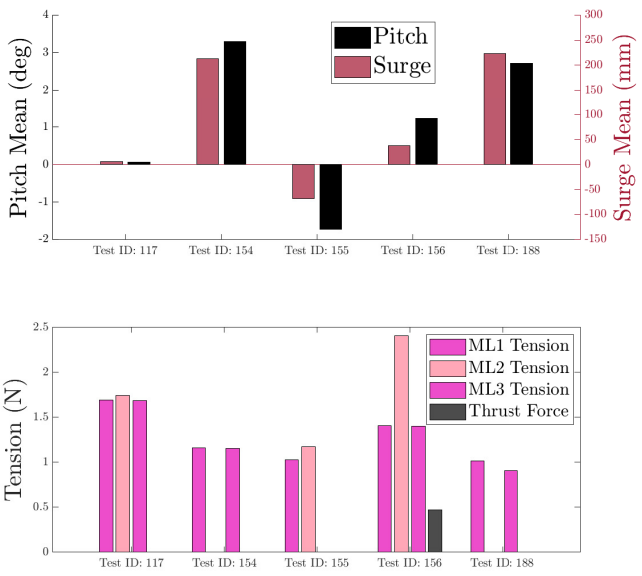

Figure 11: In the top graph of the figure, the average values of surge and pitch for the 5 tests are shown. In the bottom graph, the tensions on the mooring lines and the aerodynamic force applied by the actuator line (when present) are depicted.

tial rupture. Therefore, the design of the mooring line must ensure that this excess tension does not exceed the minimum breaking load of the line. Regarding the motions of the structure, there are no significant differences compared to the undamaged case, as the global stiffness properties of the mooring remain unchanged. This occurs in mooring configurations with constant stiffness, such as those with springs. However, if the stiffness of the lines varies with load, as in the case of nylon lines, the same conclusion cannot be drawn. This will be the subject of future tests. The failure test with nylon lines reproduces the rupture of the bow line. In this case, although the average tension decreases, the maximum tensions are

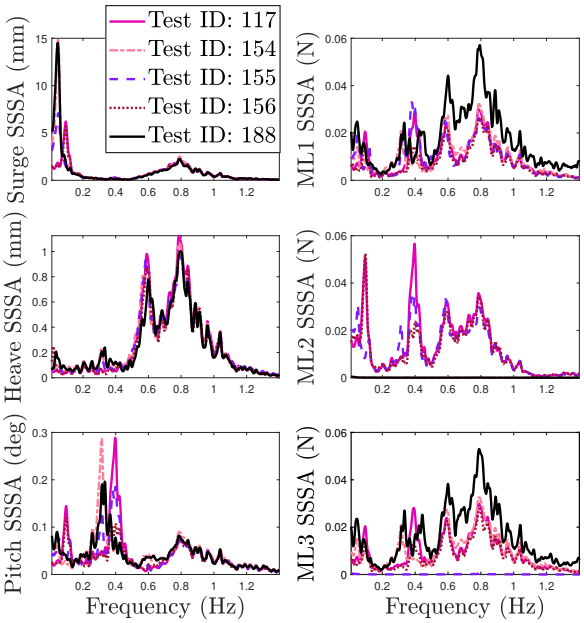

Figure 12: The figure shows the Single Side Spectrum Amplitude (SSSA) of the surge, heave, and pitch motions, as well as the tensions on the 3 mooring lines. The SSSA values are displayed for each of the 5 tests conducted during the experimental campaign.

higher compared to the configuration with springs. This happens because when the tension increases, the line stiffens, leading to higher peak tensions. In the future, we aim to investigate the configuration with only nylon lines more thoroughly. Additionally, we plan to test this system on larger scales, where it is easier to precisely replicate the stiffness of the lines at full scale. In this work, the 1:96 scale is limiting, especially in this regard.

REFERENCES

Bach-Gansmo, M. T., S. K. Garvik, J. B. Thomsen, & M. T. Andersen (2020). Parametric study of a taut compliant mooring system for a fowt compared to a catenary mooring. *Journal of Marine Science and Engineering 8*(6), 431.

ERA5. Era5 database. Available online: `https://cds.climate.copernicus.eu/cdsapp#!/dataset/reanalysis-era5-single-levels?tab=form`, Accessed on May 08, 2024.

Falkenberg, E., L. Yang, & V. Åhjem (2018, 06). The syrope method for stiffness testing of polyester ropes. In *International Conference on Offshore Mechanics and Arctic Engineering*, Volume Volume 1: Offshore Technology, pp. V001T01A067.

Hersbach, H., B. Bell, P. Berrisford, S. Hirahara, A. Horányi, J. Muñoz-Sabater, J. Nicolas, C. Peubey, R. Radu, & D. Schepers (2020). The era5 global reanalysis. *Quarterly Journal of the Royal Meteorological Society 146*(730), 1999–2049.

ITTC, H. (2014). Guide to the expression of uncertainty in experimental hydrodynamics.

Jonkman, J., S. Butterfield, W. Musial, & G. Scott (2009). Definition of a 5-mw reference wind turbine for offshore system development.

LeeSpring. Leespring. Available online: `https://www.leespring.de/en`, Accessed on May 08, 2024.

Niosi, F., E. Begovic, C. Bertorello, B. Rinauro, G. Sannino, M. Bonfanti, & S. A. Sirigu (2023). Experimental validation of orcaflex-based numerical models for the pewec device. *Ocean Engineering 281*, 114963.

Niosi, F., L. Parrinello, B. Paduano, E. Pasta, F. Carapellese, & G. Bracco (2021). On the influence of mooring in wave energy converters productivity: the pewec case. In *2021 International Conference on Electrical, Computer, Communications and Mechatronics Engineering (ICECCME)*, pp. 1–6.

Orcina. Orcaflex. Available online: `www.orcina.com/webhelp/OrcaFlex/`, Accessed on September 15th, 2023.

Paduano, B., L. Parrinello, F. Niosi, O. Dell'Edera, S. A. Sirigu, N. Faedo, & G. Mattiazzo (2024). Towards standardised design of wave energy converters: A high-fidelity modelling approach. *Renewable Energy 224*, 120141.

Robertson, A., J. Jonkman, M. Masciola, H. Song, A. Goupee, A. Coulling, & C. Luan (2014). Definition of the semisubmersible floating system for phase ii of oc4. Technical report, National Renewable Energy Lab.(NREL), Golden, CO (United States).

Veritas, D. N. & G. Lloyd (2017). Recommended practice for design, testing and analysis of offshore fibre ropes (dnvgl-rp-e305).

Wang, H. (2022). *Taut Mooring*, pp. 1933–1937. Singapore: Springer Nature Singapore.